Title

Thermal Transitions in Perfluorosulfonated Ionomer Thin-Films

Journal

ACS MACRO LETTERS, 7(10)

Authors

Tesfaye, Meron
Kushner, Douglas I
McCloskey, Bryan D
et al.

Publication Date

2018

DOI

10.1021/acsmacrolett.8b00628

Thermal Transitions in Perfluorosulfonated Ionomer Thin-Films

Meron Tesfaye [a, b, *], Douglas Kushner [b], Bryan D. McCloskey [a, b], Adam Z. Weber [b], Ahmet Kusoglu[b]

[a] Chemical and Biomolecular Engineering, University of California Berkeley, Berkeley, CA, 94720

[b] Energy Technologies Area, Lawrence Berkeley National Laboratory, Berkeley, CA, 94720

* Author to whom correspondence should be addressed: mtesfaye@berkeley.edu

Abstract

Thin perfluorosulfonated ion-conducting polymers (PFSI ionomers) in energy-conversion devices have limitations in functionality attributed to confinement-driven and surface-dependent interactions. This study highlights the effects of confinement and interface-dependent interactions of PFSI thin-films on gas transport by exploring thin-film thermal transition temperature (T_T). Change in T_T is a key marker of stiffness and chain mobility and has direct implications on gas transport through polymer films. This work demonstrates an increase in the T_T with decreasing PFSI film thickness in acid (H^+) form (from 70 to 130°C for 400 to 10 nm, respectively). In metal (M^+) cation exchanged PFSI, T_T remained constant with thickness. Results point to an interplay between increased chain mobility at the free surface and hindered motion at the substrate interface, which is amplified upon confinement. This balance is impacted by ionomer intermolecular forces as strong ionic crosslinking within the PFSI-M^+ matrix raises the transition temperature over the mainly hydrogen bonded PFSI-H^+ ionomer.

Table of Contents (TOC) graphic

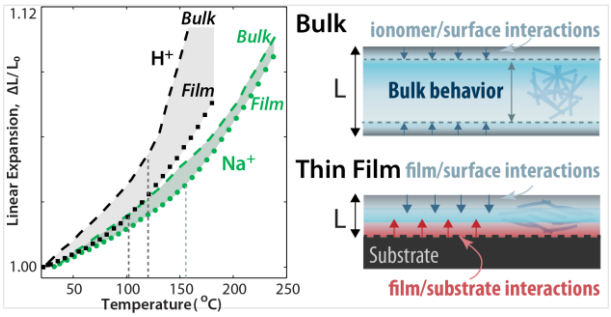

Polymer thin-films are increasingly employed in coating applications, gas-separation systems, and energy-conversion devices, expanding the ubiquitous use of polymers, reducing cost, and material waste.[1–3] However, deviation of physical properties in thin polymer films (thickness < 100 nm) compared to bulk (thickness typically >10 μm) adds significant uncertainty to their utility.[4–7] As the polymer film thickness approaches the molecular lengthscale, the influence of local surface and interface effects are amplified, resulting in thin-film structure non-uniformity, stability differences, and variations in dynamics compared to bulk behavior.[3,8,9] Such is also the case for ion-conducting polymer (ionomer) thin-films employed in polymer-electrolyte fuel cells (PEFCs) and related technologies. Perfluorosulfonated ionomer (PFSI) thin-films of 4 to 100 nm thickness are used as a solid-electrolyte binder in porous electrodes to improve catalytic activity (e.g., by creating pathways for proton transport to carbon-supported platinum in PEFC electrodes).[10,11] These thin-film ionomers behave dissimilarly from their corresponding bulk behavior, and are responsible for significant mass-transport resistances at the desired high current densities.[12–14] Studies focusing on nano-confined ionomers have demonstrated the effect of thickness and substrate on morphology and domain orientation that alter an ionomer's proton conductivity on carbon and platinum surfaces.[15–17] Additionally, changes in ionomer ion-exchange capacity (IEC, inverse of the equivalent weight (EW)), variability in processing conditions, and differences in surface wettability and interaction have already been proven to impact mechanical properties and water-uptake capacity of ionomer thin-films.[18–22] Following these trends, it is reasonable to presuppose similar nano-confinement effects on gas permeability to explain the aforementioned inferred ionomer thin-film gas-transport resistances.[23] However, a direct correlation of gas transport to confinement-driven parameters in ionomer thin-films has yet to be established.

Gas transport through dense polymers involves the dissolution of gas at the membrane surface followed by a transport process which is driven by a chemical potential gradient through the membrane and mediated by polymer chain mobility.[24] One broad physical descriptor correlating polymeric material structure with gas permeability is the glass-transition temperature, T_g. As a proxy for polymer chain relaxation and segmental motion, T_g is correlated to molecular packing and available free volume impacting the gas-transport process.[25] In a highly confined system, like that of an ionomer thin-film coating an electrocatalyst, T_g can serve as a characteristic thermodynamic transition of structural relaxation correlating confinement with gas transport.[3] Thus, quantifying the transition temperature and elucidating the interplay between chain mobility and gas transport in nano-confined ionomers is the focus of this study.

A major challenge in utilizing T_g as a single marker for relaxation behavior, as is frequently done in neutral homopolymers, is the presence of multiple thermal transitions (T_T's) in bulk PFSI and their long-debated nature and source.[26–28] PFSIs are random copolymers composed of hydrophobic tetrafluoroethylene backbone units and perfluorovinyl ether side chains containing an ionic end group $–SO_3H$.[29,30] A consequence of this nanophase separated, complex ionic structure is the presence of four thermal transitions (γ, β', β, α) that describe the mechanical and relaxation behavior of PFSI. T_γ (–100 to –80°C) occurs due to local short-range motion in the backbone $-CF_2-$ chains independent of counterion type (SO_3-M).[26,28] β' and β relaxation have been attributed to ether side-chain motion and main-chain motion in PFSI network, respectively.[28,31] T_β relaxation is considered equivalent to the T_g in classical glassy polymers, which marks the onset of transition from glassy (brittle) to rubbery (viscous) behavior. For hydrogen-bonded PFSI in H^+ form, β relaxations have been reported to be around –60 to 23ºC.[29] However, exchanging H^+ with different counterions (M^+) results in distinct dynamic-mechanical analysis peaks for the ether side-chain $T_{\beta'}$ (near –20 to –30°C) and ionomer

matrix, T_β (around 130 to 170°C).[27,28] The final thermal transition, α-relaxation, T_α (87 to 120°C in H^+ form and 210 to 240°C in various M^+ form),[32,33] is attributed to relaxation of the clustered ionic domains scattered within the nonpolar ionomer matrix. Although the transition temperatures are discussed as distinct relaxations, they are likely to have coupled influence on gas permeation by impacting segmental mobility, intramolecular packing, and free volume.[24] Taking this fact into account, this study aims to develop understanding of confinement-driven changes in gas transport of PFSIs (Nafion and 3M PFSA) via transition temperature measurements in the 30 to 250°C range, simply referred to as T_T herein. Using supported ionomer thin-film model systems, the dependence of T_T on intermolecular forces and chain mobility is explored via metal counterion exchange (Na^+, Cs^+).

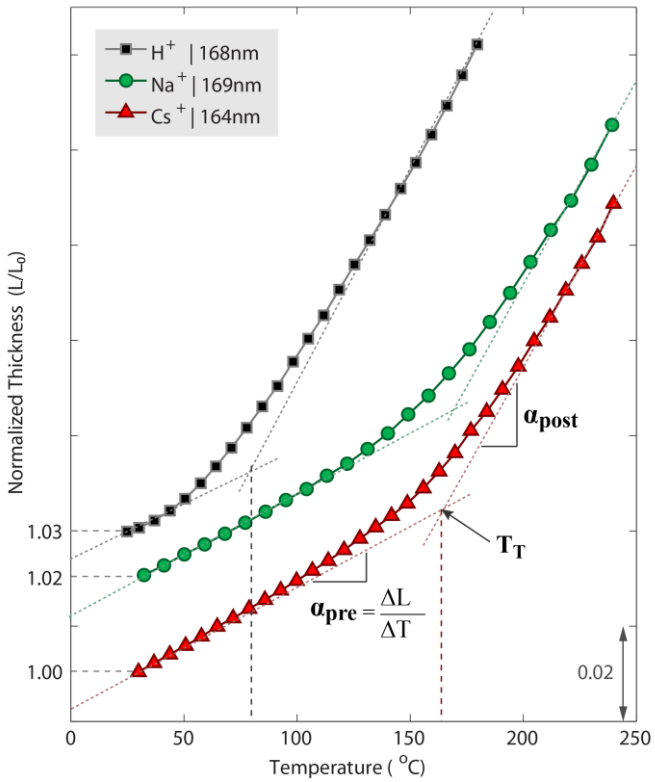

Figure 1: Change in normalized thickness (L/L_o) with respect to dry thickness(L_o) during cooling used for calculating transition temperature (T_T) and pre- and post- transition expansion rate (α_{pre} and α_{post}). Curves are offset in the y-axis for improved visibility.

T_T in thin-film polymers can be obtained via volume expansion,[34] segmental mobility,[35] and viscoelasticity[36] tracking techniques. Fig. 1 shows normalized thickness profile of Nafion thin-films in acid (H^+) and cationic (Na^+ and Cs^+) forms obtained via *in-situ* heated cell ellipsometry (see expanded details in SI). A change in the rate of thickness expansion at a specific temperature is defined as the PFSI T_T. Linear thermal-expansion coefficients (α_L) in pre- and post-transition temperature regimes are calculated via

$$\alpha_L = \frac{1}{L_o}\frac{\Delta L}{\Delta T} \quad (1)$$

where L_o is the ambient, dry thickness and ΔL and ΔT represent change in thickness and temperature, respectively. Fig. 2 shows T_T and pre- and post- α_L of PFSI-H^+ as a function of thickness, extracted from similar measurements shown in Fig. 1. This 1-dimensional α_L is compared to isotropic, 3-dimensional average volumetric thermal-expansion coefficient (α_V) of bulk PFSI to provide context, where $\alpha_V \approx 3 \cdot \alpha_{L,bulk}$.[37] Both thin-film T_T and α_L demonstrate no significant correlation with PFSI EW (see Fig. 2). The relative difference between pre- and post-expansion rate and range of T_T observed for thin-film PFSI-H^+ indicates that T_T is likely T_α. The T_T of thin-film ionomers > 100 nm in Fig. 2a are lower than T_α of cast bulk Nafion in H^+ form (~87 °C),[29,38] and an increase in T_T with decreasing thickness is observed with some data variability. α_{pre} remains somewhat constant while α_{post} decreases with decreasing thickness (Fig. 2b), consistent with the raised T_T evaluated. Thermal transition and subsequent relaxation behavior in thin-film polymers is governed by chain conformation upon confinement, polymer dynamics at the free-surface/polymer, and substrate/polymer interfacial interactions.[39] It is well documented that polymer chains adsorbed at attractive interfaces induce changes in orientation and local packing that results in a decreasing polymer density distribution away from the surface.[40,41] Spatially opposite to the polymer/substrate interface, the free-surface/polymer interface has unhindered mobility and enhanced configurational freedom, thereby improving long-

range motions and lowering the transition temperature.[42–44] High wettability and low surface energy of the Si/SiO_2 support results in favorable adsorption of the PFSI-H^+ side-chain moieties[45,46] resulting in pinned ionomer chains and increased local packing at the ionomer/substrate interface.

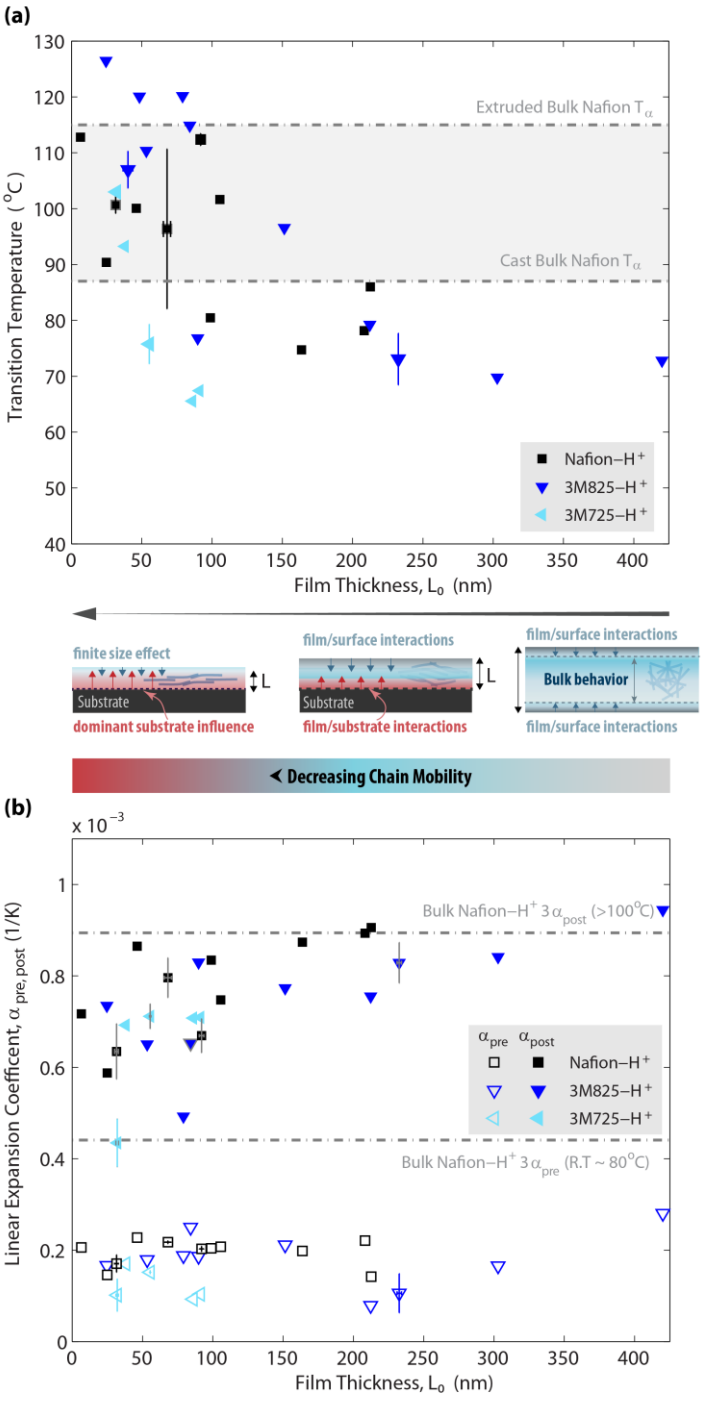

Figure 2: (a) Transition temperature and (b) Linear expansion coefficient, α_{pre} and α_{post}, of thin-film PFSI-H+ cast on Si/SiO_2 substrate compared to bulk Nafion linear expansion from Ref. [47]

As a result, PFSI-H^+ thin-films have significantly restricted chain mobility below the T_T, as is reflected by the low α_{pre} as illustrated in the schematics in Fig. 2. As the temperature exceeds T_T, entropically-frozen ionomer chains gain enough thermal energy (kT) to break electrostatic interactions between PFSI-H^+ side-chains and substrate, thereby relaxing the substrate-imposed constraints and resulting in an α_{post} similar to bulk PFSI. With a further decrease in thickness, the relative contribution of substrate interaction is amplified, resulting in a positive shift in T_T.

Fig. 3 shows T_T, α_{pre}, and α_{post} of ionomer thin-film in Na^+ and Cs^+ form as well as bulk film. Both α_{pre} and α_{post} are similar to the expansion rates observed in bulk Nafion around the β transition.[47] Here, unlike the PFSI-H^+ for which T_T was assigned to the α transition, the T_T for PFSI-M^+ is attributed to the β transition due to (1) only a single transition temperature observed for PFSI-M^+ thin-films and (2) the large positive shift (> 100ºC) expected in both T_α and T_β with neutralization, as reported extensively in bulk PFSI literature and as discussed above.[26,31,48] PFSI-M^+ exhibit very small deviation from bulk T_β in the range of film thicknesses explored, contrary to PFSI-H^+ (Fig. 3a). Table 1 compares PFSI T_α and T_β reported in literature with substrate-supported thin-film PFSI T_T measured in this study. Although T_T measured in PFSI-H^+ and PFSI-M^+ are speculated to be T_α and T_β respectively, detailed spectroscopic and x-ray scattering studies are needed to confirm.

Table 1: Comparison of literature reported transition temperatures (T_T) for bulk PFSI in different forms and thin-film thermal transitions observed in this study.

	T_β	T_α	Ref.
PFSI-H+ (Bulk film)	−20 to −30°C	87 to 115 ºC	[27–32]
PFSI-M+ (Bulk film)	130 to 170°C	210 to 240°C	
PFSI-H+ (Thin-film)			
>100nm	T_T n.o.	70 to 85°C	This work.
<100nm		70 to 130°C	
PFSI-M+ (Thin-film)			
>100nm	160 to 170°C	T_T n.o.	This work.
<100nm	160 to 170°C		

T_T n.o. = thermal transition temperature not observed in this study.

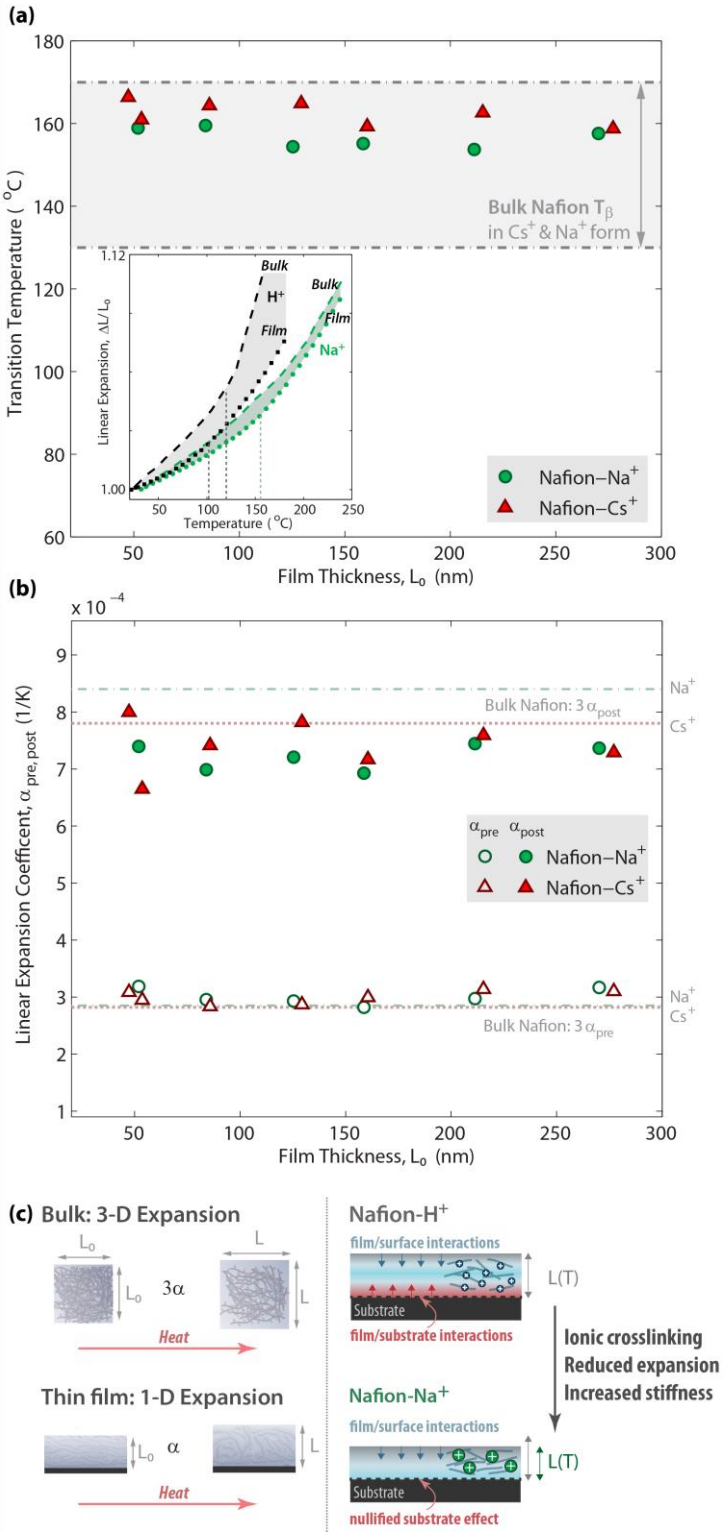

Figure 3: (a) Transition temperature and (inset) bulk vs. thin-film linear expansion PFSI-H^+ vs. PFSI-Na^+ form (b) Linear expansion coefficient, α_{pre} and α_{post}, of thin-film PFSI-Na^+ and PFSI-Cs^+ cast on Si/SiO_2 substrate, compared to bulk Nafion linear expansion from Ref. [47] (c) Illustration of comparative volumetric expansion of PFSI in bulk vs. thin-film and proton (H^+) vs. cation (Na^+) form.

At this point, it is critical to evaluate results discussed in Fig. 2 and Fig. 3 as complementary portrayal of the segmental mobility dynamics found in PFSI thin-films. High mobility near the free-surface/ionomer interface reduces T_T of PFSI-H^+ thin-films >100 nm relative to bulk as represented schematically in Fig. 2. Upon continued confinement to thicknesses below 100 nm, PFSI-H^+ thin-film T_T increases due to amplified impact of substrate interaction, likely through strong hydrogen bonding between the substrate and PFSI-H^+. Addition of metal cations increases the strength of ionic crosslinking in PFSI-M^+ matrix, resulting in reduced conformational relaxation and subsequent increase in T_T, as depicted in Fig. 3c. Presumably, strong ion-polymer intermolecular interactions in PFSI-M^+ appear to nullify substrate/ionomer interactions upon confinement such that T_T, α_{pre}, and α_{post} are similar to bulk PFSI-M^+ values regardless of film thickness.

This work is the first time spectroscopic ellipsometry was employed to evaluate thermal transitions in PFSI. Findings in this study confirm the strong influence of substrate and free surface upon confinement witnessed in neutralized polymer thin-films.[3,8,42,49] Increasing T_T with confinement and presence of large univalent counterion points to increased ionomer chain stiffness that could result in reduced gas permeability (see illustrations in Fig. 2 and Fig. 3). In agreement with our findings, a study focusing on Cs^+ and Pt^{2+} ion-exchanged Nafion by Mohamed et al. showed greater free volume thermal expansion in H^+ form.[50] They also revealed chain-stiffening-induced reduction in gas permeation with counterion exchange despite the higher free volume measured. Confinement and counterion induced chain stiffening has been observed with rise in modulus relative to bulk PFSI and PFSI-H^+ moduli, respectively.[20,33,51,52] Although the polymer thickness at which the confinement effect commences does not always directly correlate with transition-temperature deviation from the bulk value, the trend in T_g is in accord with the trends in moduli of various thin-film polymers.[6,53] Similarly, confined (< 100 nm) and cation-exchanged PFSI appear to have impeded chain mobility

and increased stiffness induced by substrate and ionic-crosslinking, as evidenced by their higher T_T, that can ultimately result in reduced gas permeability. Additionally, the magnitude of $T-T_T$ can serve as a proxy for ionomer mobility. A decrease in oxygen permeability with decreasing PFSI thin-film thickness demonstrated in literature[13,14] tracks closely with $T-T_T$ measured in this study for a given thickness. The utilized ellipsometry technique employs a single variable (thickness variation) to characterize local changes in mobility, which could be delineated further with complementary methods tracking changes in ionomer density and synergistic spectroscopic techniques that can probe molecular fluctuations. Findings in this letter signify the interplay between the substrate interactions and ionic interactions controlling the thermal transitions in confined ionomer films, which could be harnessed to understand and tune ionomers' gas transport properties and their functionality in porous electrodes of electrochemical energy conversion devices.

Acknowledgements

We thank Andrew Haug and Michael Yandrasits of 3M for providing us with the PFSA dispersions and Micheal Gerhardt for helpful insights and discussions. This work made use of facilities at the Joint Center for Artificial Photosynthesis, a DOE Energy Innovation Hub, supported through the Office of Science of the U.S. Department of Energy under Award Number DE-SC0004993. Funding support was supplied in part by the National Science Foundation (Grant No. DGE 1106400) and the Fuel Cell Performance and Durability Consortium (FC-PAD), by the Fuel Cell Technologies Office (FCTO), Office of Energy Efficiency and Renewable Energy (EERE), of the U.S. Department of Energy under contract number DE-AC02-05CH11231. †

Supporting Information:

Expanded experimental details are provided as Supporting Information.

References

(1) Brauman, J. I.; Szuromi, P. Thin Films. *Science (80-.).* **1996**, *273* (5277), 855 LP-855.

(2) C. W. Frank, V. Rao, M. M. Despotopoulou, R. F. W. Pease, W. D. Hinsberg, R. D. M. and J. F. R. Structure in Thin and Ultrathin Spin-Cast Polymer Films. *Science (80-.).* **1996**, *273*.

(3) Alcoutlabi, M.; McKenna, G. B. Effects of Confinement on Material Behaviour at the Nanometre Size Scale. *J. Phys. Condens. Matter* **2005**, *17* (15).

(4) Rowe, B. W.; Freeman, B. D.; Paul, D. R. Physical Aging of Ultrathin Glassy Polymer Films Tracked by Gas Permeability. *Polymer (Guildf).* **2009**, *50* (23), 5565–5575.

(5) Rittigstein, P.; Priestley, R. D.; Broadbelt, L. J.; Torkelson, J. M. Model Polymer Nanocomposites Provide an Understanding of Confinement Effects in Real Nanocomposites. *Nat. Mater.* **2007**, *6* (4), 278–282.

(6) Torres, J. M.; Stafford, C. M.; Vogt, B. D. Elastic Modulus of Amorphous Polymer Thin Films: Relationship to the Glass Transition Temperature. *ACS Nano* **2009**, *3* (9), 2677–2685.

(7) Harry D. Rowland, William P. King, John B. Pethica, G. L. W. C. Molecular Confinement Accelerates Deformation of Entangled Polymers During Squeeze Flow. *Science (80-.).* **2008**, *322*, 720–724.

(8) Russell, T. P.; Chai, Y. 50th Anniversary Perspective: Putting the Squeeze on Polymers: A Perspective on Polymer Thin Films and Interfaces. *Macromolecules* **2017**, *50* (12), 4597–4609.

(9) Napolitano, S.; Glynos, E.; Tito, N. B. Glass Transition of Polymers in Bulk, Confined Geometries, and near Interfaces. *Reports Prog. Phys.* **2017**, *80* (3).

(10) Gottesfeld, S. Oxygen Reduction Kinetics on a Platinum RDE Coated with a Recast Nafion Film. *J. Electrochem. Soc.* **1987**, *134* (6), 1455.

(11) Parthasarthy, A.; Srinivasan, S.; Appleby, A. J.; Martin, C. R. Electrode-Kinetics of Oxygen

Reduction at Carbon-Supported and Unsupported Platinum Microcrystallite Nafion(R) Interfaces. *J. Electroanal. Chem.* **1992**, *339* (1–2), 101–121.

(12) Nonoyama, N.; Okazaki, S.; Weber, A. Z.; Ikogi, Y.; Yoshida, T. Analysis of Oxygen-Transport Diffusion Resistance in Proton-Exchange-Membrane Fuel Cells. *J. Electrochem. Soc.* **2011**, *158* (4), B416.

(13) Kudo, K.; Jinnouchi, R.; Morimoto, Y. Humidity and Temperature Dependences of Oxygen Transport Resistance of Nafion Thin Film on Platinum Electrode. *Electrochim. Acta* **2016**, *209*, 682–690.

(14) Suzuki, T.; Kudo, K.; Morimoto, Y. Model for Investigation of Oxygen Transport Limitation in a Polymer Electrolyte Fuel Cell. *J. Power Sources* **2013**, *222*, 379–389.

(15) Ohira, A.; Kuroda, S.; Mohamedz, H. F. M.; Tavernier, B. Effect of Interface on Surface Morphology and Proton Conduction of Polymer Electrolyte Thin Films. *Phys. Chem. Chem. Phys. Phys. Chem. Chem. Phys* **2013**, *15*, 11494–11500.

(16) Kusoglu, A.; Kushner, D.; Paul, D. K.; Karan, K.; Hickner, M. a.; Weber, A. Z. Impact of Substrate and Processing on Confi Nement of Nafi on Thin Films. *Adv. Funct. Mater.* **2014**, *24* (30), 4763–4774.

(17) Nagao, Y. Proton-Conductivity Enhancement in Polymer Thin Films. *Langmuir* **2017**, acs.langmuir.7b01484.

(18) Kusoglu, A.; Dursch, T. J.; Weber, A. Z. Nanostructure/Swelling Relationships of Bulk and Thin-Film PFSA Ionomers. *Adv. Funct. Mater.* **2016**, *26* (27), 4961–4975.

(19) Frieberg, B. R.; Page, K. A.; Graybill, J. R.; Walker, M. L.; Stafford, C. M.; Stafford, G. R.; Soles, C. L. Mechanical Response of Thermally Annealed Nafion Thin Films. *ACS Appl. Mater. Interfaces* **2016**, *8* (48), 33240–33249.

(20) Page, K. A.; Kusoglu, A.; Stafford, C. M.; Kim, S.; Kline, R. J.; Weber, A. Z. Confinement-Driven Increase in Ionomer Thin-Film Modulus. *Nano Lett.* **2014**, *14* (5), 2299–2304.

(21) Paul, D. K.; Shim, H. K. K.; Giorgi, J. B.; Karan, K. Thickness Dependence of Thermally Induced Changes in Surface and Bulk Properties of Nafion ® Nanofilms. *J. Polym. Sci. Part B Polym. Phys.* **2016**, *54* (13), 1267–1277.

(22) Tesfaye, M.; MacDonald, A. N.; Dudenas, P. J.; Kusoglu, A.; Weber, A. Z. Exploring Substrate/Ionomer Interaction under Oxidizing and Reducing Environments. *Electrochem. commun.* **2018**, *87* (January), 86–90.

(23) Weber, A. Z.; Kusoglu, A. Unexplained Transport Resistances for Low-Loaded Fuel-Cell Catalyst Layers. *J. Mater. Chem. A* **2014**, *2* (c), 17207–17211.

(24) Yampolskii, Y.; Pinnau, I.; Freeman, B. D. *Materials Science of Membranes for Gas and Vapor Separation*; 2006.

(25) Fried, J. R.; Sadat-Akhavi, M.; Mark, J. E. Molecular Simulation of Gas Permeability: Poly(2,6-Dimethyl-1,4-Phenylene Oxide). *J. Memb. Sci.* **1998**, *149* (1), 115–126.

(26) Osborn, S. J.; Hassan, M. K.; Divoux, G. M.; Rhoades, D. W.; Mauritz, K. a.; Moore, R. B. Glass Transition Temperature of Perfluorosulfonic Acid Ionomers. *Macromolecules* **2007**, *40* (10), 3886–3890.

(27) Matos, B. R.; Dresch, M. A.; Santiago, E. I.; Linardi, M.; de Florio, D. Z.; Fonseca, F. C. Nafion -Relaxation Dependence on Temperature and Relative Humidity Studied by Dielectric Spectroscopy. *J. Electrochem. Soc.* **2012**, *160* (1), F43–F48.

(28) Kyu, T.; Hashiyama, M.; Eisenberg, A. Dynamic Mechanical Studies of Partially Ionized and Neutralized Nafion Polymers. *Can. J. Chem.* **1983**, *61*, 680–687.

(29) Kusoglu, A.; Weber, A. Z. New Insights into Perfluorinated Sulfonic-Acid Ionomers. *Chem.*

Rev. **2017**, *117* (3), 987–1104.

(30) Mauritz, K. a; Moore, R. B. State of Understanding of Nafion. *Chem. Rev.* **2004**, *104* (10), 4535–4585.

(31) Page, K. A.; Landis, F. A.; Phillips, A. K.; Moore, R. B. SAXS Analysis of the Thermal Relaxation of Anisotropic Morphologies in Oriented Nafion Membranes. *Macromolecules* **2006**, *39* (11), 3939–3946.

(32) Fan, Y.; Tongren, D.; Cornelius, C. J. The Role of a Metal Ion within Nafion upon Its Physical and Gas Transport Properties. *Eur. Polym. J.* **2014**, *50*, 271–278.

(33) Shi, S.; Weber, A. Z.; Kusoglu, A. Electrochimica Acta STRUCTURE-TRANSPORT RELATIONSHIP OF PERFLUOROSULFONIC-ACID MEMBRANES IN DIFFERENT CATIONIC FORMS. *Electrochim. Acta* **2016**, *220*, 517–528.

(34) Dalnoki-Veress, K.; Forrest, J. a; Murray, C.; Gigault, C.; Dutcher, J. R. Molecular Weight Dependence of Reductions in the Glass Transition Temperature of Thin, Freely Standing Polymer Films. *Phys. Rev. E. Stat. Nonlin. Soft Matter Phys.* **2001**, *63* (3 Pt 1), 031801.

(35) Hall, D. B.; Miller, R. D.; Torkelson, J. M. Molecular Probe Techniques for Studying Diffusion and Relaxation in Thin and Ultrathin Polymer Films. *J Polym Sci B Polym Phys* **1997**, *35*, 2795–2802.

(36) Buenviaje, C.; Dinelli, F.; Overney, R. M. Glass Transition Measurements of Ultrathin Polystyrene Films. In *Techniques*; 2000; Vol. 77, pp 1–18.

(37) Ho, C. Y.; Taylor, R. E. *Thermal Expansion of Solids*, Vol. 4.; ASM International, 1998.

(38) Transactions, E. C. S.; Society, T. E. SSC 3M Ionomer Nafion^{TM}. **2010**, *33* (1), 627–633.

(39) Hammerschmidt, J. A.; Gladfelter, W. L.; Haugstad, G. Probing Polymer Viscoelastic Relaxations with Temperature-Controlled Friction Force Microscopy. *Macromolecules* **1999**,

32 (10), 3360–3367.

(40) De Virgiliis, a; Milchev, a; Rostiashvili, V. G.; Vilgis, T. a. Structure and Dynamics of a Polymer Melt at an Attractive Surface. *Eur. Phys. J. E. Soft Matter* **2012**, *35* (9), 97.

(41) Pham, J. Q.; Green, P. F. The Glass Transition of Thin Film Polymer/Polymer Blends: Interfacial Interactions and Confinement. *J. Chem. Phys.* **2002**, *116* (13), 5801–5806.

(42) Priestley, R. D.; Ellison, C. J.; Broadbelt, L. J.; Torkelson, J. M. Structural Relaxation of Polymer Glasses at Surfaces, Interfaces, and in Between. *Science* **2005**, *309* (5733), 456–459.

(43) Burroughs, M. J.; Napolitano, S.; Cangialosi, D.; Priestley, R. D. Direct Measurement of Glass Transition Temperature in Exposed and Buried Adsorbed Polymer Nanolayers. *Macromolecules* **2016**, *49* (12), 4647–4655.

(44) Paeng, K.; Swallen, S. F.; Ediger, M. D. Direct Measurement of Molecular Motion in Freestanding Polystyrene Thin Films. *J. Am. Chem. Soc.* **2011**, *133* (22), 8444–8447.

(45) Ruhe, J.; Novotny, V.; Clarke, T.; Street, G. B. Ultrathin Perfluoropolyether Films---Influence of Anchoring and Mobility of Polymers on the Tribological Properties. *J. Tribol.* **1996**, *118* (3), 663–668.

(46) Rühe, J. G. V. J. T. G. B., Blackman, G., Novotny, V. J., Clarke, T., Street, G. B., & Kuan, S. Terminal Attachment of Perfluorinated Polymers to Solid Surfaces. *J. Appl. Polym. Sci.* **1994**, *53* (6), 825–836.

(47) Takamatsu, T.; Eisenberg, a. Density and Expansion Coefficients of Nafion. *J. App. Poly. Sci.* **1979**, *24*, 2221–2235.

(48) Yeo, S. C.; Eisenberg, A. Physical Properties and Supermolecular Structure of Perfluorinated Ion- containing (Nafion) Polymers. *J. Appl. Polym. Sci.* **1977**, *21* (4), 875–898.

(49) Priestley, R. D.; Mundra, M. K.; Barnett, N. J.; Broadbelt, L. J.; Torkelson, J. M. Effects of Nanoscale Confinement and Interfaces on the Glass Transition Temperatures of a Series of Poly(n-Methacrylate) Films. *Aust. J. Chem.* **2007**, *60* (10), 765–771.

(50) Mohamed, H. F. M.; Kobayashi, Y.; Kuroda, C. S.; Ohira, a. Free Volume and Gas Permeation in Ion-Exchanged Forms of the Nafion® Membrane. *J. Phys. Conf. Ser.* **2010**, *225*, 012038.

(51) Albe, N. D.; Bas, C.; Reymond, L.; Dane, A.; Rossinot, E.; Flandin, L. Key Counter Ion Parameters Governing Polluted Nafion Membrane Properties. *J. Polym. Sci. Part B Polym. Phys.* **2009**, *47* (14), 1381–1392.

(52) Page, K. A.; Shin, J. W.; Eastman, S. A.; Rowe, B. W.; Kim, S.; Kusoglu, A.; Yager, K. G.; Stafford, G. R. In Situ Method for Measuring the Mechanical Properties of Nafion Thin Films during Hydration Cycles. *ACS Appl. Mater. Interfaces* **2015**, *7* (32), 17874–17883.

(53) Tweedie, C. A.; Constantinides, G.; Lehman, K. E.; Brill, D. J.; Blackman, G. S.; Van Vliet, K. J. Enhanced Stiffness of Amorphous Polymer Surfaces under Confinement of Localized Contact Loads. *Adv. Mater.* **2007**, *19* (18), 2540–2546.